Please cite this article in press as: Chang et al., Targeting Amyloid-β Precursor Protein, *APP*, Splicing with Antisense Oligonucleotides Reduces Toxic Amyloid-β Production, Molecular Therapy (2018), https://doi.org/10.1016/j.ymthe.2018.02.029

Molecular Therapy
Original Article

Targeting Amyloid-β Precursor Protein, *APP*, Splicing with Antisense Oligonucleotides Reduces Toxic Amyloid-β Production

Jennifer L. Chang,[1] Anthony J. Hinrich,[1] Brandon Roman,[2] Michaela Norrbom,[3] Frank Rigo,[3] Robert A. Marr,[4] Eric M. Norstrom,[2] and Michelle L. Hastings[1]

[1]Department of Cell Biology and Anatomy, Center for Genetic Diseases, Chicago Medical School and School of Graduate and Postdoctoral Studies, Rosalind Franklin University of Medicine and Science, North Chicago, IL 60064, USA; [2]Department of Biological Sciences, DePaul University, Chicago, IL 60614, USA; [3]Ionis Pharmaceuticals, Carlsbad, CA 92010, USA; [4]Department of Neuroscience, Rosalind Franklin University of Medicine and Science, North Chicago, IL 60064, USA

Alterations in amyloid beta precursor protein (APP) have been implicated in cognitive decline in Alzheimer's disease (AD), which is accelerated in Down syndrome/Trisomy 21 (DS/TS21), likely due to the extra copy of the APP gene, located on chromosome 21. Proteolytic cleavage of APP generates amyloid-β (Aβ) peptide, the primary component of senile plaques associated with AD. Reducing Aβ production is predicted to lower plaque burden and mitigate AD symptoms. Here, we designed a splice-switching antisense oligonucleotide (SSO) that causes skipping of the APP exon that encodes proteolytic cleavage sites required for Aβ peptide production. The SSO induced exon skipping in Down syndrome cell lines, resulting in a reduction of Aβ. Treatment of mice with the SSO resulted in widespread distribution in the brain accompanied by APP exon skipping and a reduction of Aβ. Overall, we show that an alternatively spliced isoform of APP encodes a cleavage-incompetent protein that does not produce Aβ peptide and that promoting the production of this isoform with an SSO can reduce Aβ *in vivo*. These findings demonstrate the utility of using SSOs to induce a spliced isoform of APP to reduce Aβ as a potential approach for treating AD.

INTRODUCTION

Alzheimer's disease (AD) is the most prevalent neurodegenerative disorder, accounting for 60%–80% of the more than 40 million cases of dementia worldwide.[1–3] One pathological hallmark of AD is the accumulation of amyloid-β (Aβ) peptide as extracellular plaques in the brain.[4–6] Aβ is a 38- to 42-amino acid peptide that is produced by proteolysis of amyloid precursor protein, APP. Some forms of Aβ are prone to aggregation and plaque formation, which is thought to initiate a cascade of pathological events associated with the development and progression of AD.[6] Thus, targeting Aβ has been a major focus of therapeutic development for AD.[1,3,7]

APP is a member of a conserved protein family that also includes amyloid precursor-like proteins 1 and 2 (APLP1, APLP2).[8–10] The proteins in this family are type I single-pass transmembrane glycoproteins with receptor-like structural features but not entirely clear cellular functions.[11–14] These proteins have conserved structural motifs and proteolytic processing pathways and may have functional redundancy, though only APP contains the Aβ sequence associated with amyloid plaques. Two proteolytic pathways account for the majority of APP processing.[15,16] One pathway is considered non-amyloidogenic and occurs via an initial APP cleavage in the membrane-proximal region by α-secretase activity (Figure 1A).[17] The scissile bond for this activity lies within the Aβ sequence and generates an extracellular, soluble APP fragment (sAPPα) and a membrane-bound C-terminal fragment (CTFα). CTFα is a substrate for the intramembrane protease, γ-secretase, which cleaves CTFα to yield an extracellular soluble fragment, termed P3, and the intracellular APP domain (AICD). Because α-secretase cleavage occurs within the Aβ sequence, this pathway precludes generation of the Aβ peptide. The second, amyloidogenic pathway, involves β-secretase (BACE1) cleavage of APP to liberate a soluble peptide (sAPPβ). The remaining membrane-bound C-terminal fragment (CTFβ) is subsequently cleaved by γ-secretase, generating the Aβ peptide and AICD.[18–20] γ-Secretase cleaves CTFβ at multiple sites, essentially trimming the peptide into shorter, more soluble and benign forms of Aβ.[21] While the primary species of Aβ is the 40-amino-acid form (Aβ40), inefficient cleavage can result in the release of the longer and more aggregation-prone Aβ42, which is associated with neurotoxic amyloid plaque formation.[20,22] Because of their role in the generation of Aβ, β- and γ-secretase inhibitors have been a major focus of drug development for AD, though therapeutically targeting these proteases has been challenging.[23,24]

Evidence supporting a direct role for APP and Aβ in the development of AD comes from cases of autosomal-dominant forms of early-onset

Received 22 January 2018; accepted 27 February 2018;
https://doi.org/10.1016/j.ymthe.2018.02.029.

Correspondence: Michelle L. Hastings, Department of Cell Biology and Anatomy, The Chicago Medical School, Rosalind Franklin University of Medicine and Science, 3333 Green Bay Drive, North Chicago, IL 60064, USA.
E-mail: michelle.hastings@rosalindfranklin.edu

Please cite this article in press as: Chang et al., Targeting Amyloid-β Precursor Protein, *APP*, Splicing with Antisense Oligonucleotides Reduces Toxic Amyloid-β Production, Molecular Therapy (2018), https://doi.org/10.1016/j.ymthe.2018.02.029

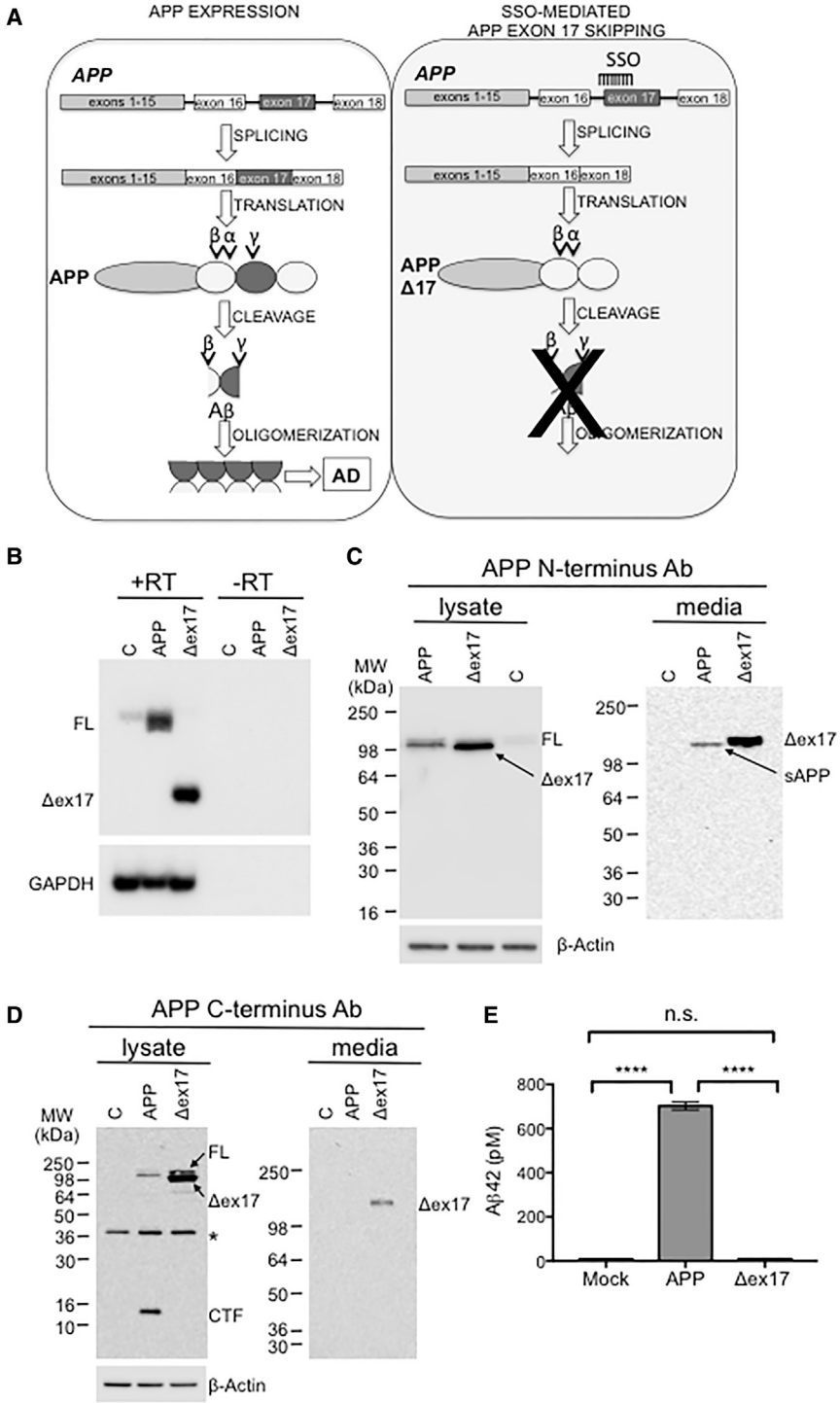

Figure 1. Deletion of APP Exon 17 Eliminates Aβ Production

(A) Schematic of reducing Aβ production and oligomerization associated with AD by using SSOs to cause APP exon 17 splicing, thereby eliminating the γ-secretase cleavage sites encoded by the exon. Arrowheads indicate the α-, β-, and γ-secretase cleavage sites encoded by exons 16, 17, and 18. Exon 17 encodes amino acids within the transmembrane domain (TM) and γ-secretase cleavage sites required for Aβ release from the membrane. Boxes represent exons, lines are introns, and ovals depict protein. (B) RT-PCR analysis of mRNA from HEK293T cells transfected with plasmids that express full-length human APP with the Swedish and Indiana mutations (APP) or APP lacking exon 17 (Δex17). RNA from mock-transfected cells was analyzed as a control to detect endogenous APP. APP was normalized to *GAPDH* to assess expression. Full-length (FL) and Δex17 refers to APP mRNA that includes or lacks exon 17, respectively. + and − RT indicates addition or omission of reverse transcriptase from the reaction, respectively. Immunoblot of APP with an antibody to detect the (C) N terminus or (D) C terminus of the protein in lysate or culture media from cells transfected with APP or APPΔex17 expression plasmids. FL designates full-length mature APP, and Δex17 refers to the protein produced from APPΔex17. The putative soluble form of APP (sAPP) that is released into the extracellular environment following secretase cleavage and the C-terminal fragment (CTF) that remains in cells after cleavage are labeled. * represents a nonspecific protein band. (E) ELISA analysis of Aβ42 abundance in media from HEK293T cells transfected with the APP or APPΔ17 plasmid. Mean Aβ42 levels for each group are graphed (±SEM; ****$p < 0.0001$, one-way ANOVA with Tukey's multiple comparisons test; $n = 2$).

familial AD (eFAD/early onset AD [EOAD]), which are associated with mutations in APP or components of the γ-secretase enzyme (PSEN1 and PSEN2). These mutations alter APP cleavage resulting in an increase in total Aβ production or the ratio of Aβ42:Aβ40.[7,25,26] Furthermore, genetic variants in proteins involved in APP cleavage can increase the risk of late-onset AD (LOAD).[27] In addition, a mutation in APP that decreases β-secretase cleavage protects against the development of AD.[28] A direct role for APP in AD is also suggested by the high incidence of the disease in individuals with Down syndrome/Trisomy 21 (DS/Ts21), a phenomenon that has been widely attributed to the presence of three copies of APP, which is located on chromosome 21.[29,30] APP expression has also been associated with traumatic brain injury (TBI) and has been suggested as a key factor in the development of dementia resulting from repeated injury.[3,31,32] Although distinguished by their genetic or environmental causes and time of onset, all of these forms of AD as well as LOAD, which has risk factors but no known single genetic cause,[33,34] are considered to be the same disease with a similar sequence of symptoms and impairments. Given the overwhelming evidence for a function of APP and Aβ production in AD, strategies to downregulate APP expression or the production of Aβ are expected to have therapeutic value in disease treatment.

Please cite this article in press as: Chang et al., Targeting Amyloid-β Precursor Protein, *APP*, Splicing with Antisense Oligonucleotides Reduces Toxic Amyloid-β Production, Molecular Therapy (2018), https://doi.org/10.1016/j.ymthe.2018.02.029

Here, we develop a new approach for targeting APP in AD using splice-switching antisense oligonucleotides (SSOs) that specifically target and modulate APP expression in a manner that reduces Aβ production. SSOs are short, single-stranded antisense oligonucleotides (ASOs) that are designed to form Watson-Crick base pairs with a specific RNA target. SSOs can be designed to base-pair to pre-mRNA and block interactions between RNA and RNA-binding proteins involved in splicing.[35,36] In this way, the SSOs can alter splice-site recognition and modulate splicing in a directed manner. SSOs are distinct from RNase H targeting ASOs, which result in degradation of the targeted RNA. Our SSOs have 2′-*O*-methoxyethyl-ribose nucleotides and a phosphorothioate-modified backbone, are water soluble, resistant to exonucleases, and highly diffusible.[37] SSOs can be delivered to the brain by intracerebroventricular (i.c.v.) injection, thereby targeting the cells of interest and limiting dose and systemic exposure. SSOs delivered in this way have widespread distribution and cellular uptake and have a remarkably long duration of action.[38] For these reasons, SSOs are not only useful as research tools for manipulation of gene expression, they are also a favorable therapeutic platform that has been developed for the treatment of disease.[36,39] An SSO drug (Spinraza; Biogen) has recently been approved by the Food and Drug Administration for the pediatric neurodegenerative disease spinal muscular atrophy.[40–42]

We designed SSOs that block *APP* exon 17 splicing and induce the production of an alternatively spliced *APP* mRNA lacking exon 17 (APPΔex17). *APPΔex17* mRNA encodes an APP protein isoform that lacks 49 amino acids including the γ-secretase cleavage sites that give rise to the toxic, AD-associated Aβ42 peptide. We confirmed that APPΔex17 does not produce Aβ42 and demonstrate SSO-induced skipping of APP exon 17 in Down syndrome fibroblast cell lines. These DS fibroblasts overexpress APP mRNA and protein and produce more Aβ42 than karyotypically normal fibroblast cells as a result of the presence of three APP genes. Our APP-targeted SSO reduced the amount of Aβ42 secreted by these cells demonstrating that APP lacking exon 17-encoded amino acids cannot be cleaved to produce Aβ42. The SSO also induced long-term suppression of *APP* exon 15 splicing in mice, the exon in mouse *APP* encoding the γ-secretase cleavage sites, and resulted in a dramatic reduction in Aβ42. Together, our results demonstrate that SSOs can induce alternatively spliced isoforms of APP that reduce amyloidogenic Aβ42. This SSO-based approach to reducing Aβ may be therapeutically beneficial in cases of dementia associated with alterations in APP abundance or activity.

RESULTS

APP Lacking Exon 17-Encoded Amino Acids Does Not Produce Aβ Peptide

Exon 17 of human *APP* encodes γ-secretase cleavage sites.[21] Removal of exon 17 from *APP* mRNA results in an in-frame deletion of 49 amino acids that leaves the α- and β-secretase cleavage sites intact and eliminates the γ-secretase sites. Thus, the resulting APP isoform lacking the sequence encoded by exon 17 (APPΔex17) cannot produce Aβ (Figure 1A). To confirm the predicted proteolytic processing of APPΔex17, we expressed cDNA encoding either the full-length APP (APP-FL) or the APPΔex17 isoform from plasmids transfected into HEK293T cells and analyzed the resulting *APP* mRNA and protein products. Cells transfected with APP-FL and APPΔex17 produced similar amounts of mRNA, which was in excess over the endogenous mRNA levels (Figure 1B). To examine APP protein and its metabolites, we used first an antibody that recognizes the N terminus of the protein.[43] APP-FL produced a protein product consistent in size to that expected of APP (Figure 1C). Expression of APPΔex17 resulted in the production of a cellular protein that migrated faster than the APP-FL protein by gel electrophoresis, consistent with the deletion of the 49 amino acids encoded by exon 17 (Figure 1C, left). The APPΔex17 was not only detected in cell lysates, but also in culture media (Figure 1C, right), suggesting that APPΔex17 is released from cells, as expected due to the deletion of the transmembrane domain. Whereas APP-FL in cell lysates is larger than APPΔex17, the APP detected in the culture media from cells transfected with APP-FL migrates faster than the APPΔex17 protein product in the media. This result is consistent with the release of soluble forms of APP (sAPPα and sAPPβ), which lack the entire C-terminal fragment domain after cleavage by α- or β-secretases. In contrast, there is no apparent shift in the migration of APPΔex17. The presence of an apparently unprocessed APPΔex17 in the culture media implies that the protein is released from the cell intact (Figure 1C).

To further characterize APP-FL and APPΔex17 cleavage, we performed immunoblot analysis of APP protein products using an antibody that recognizes the APP C terminus.[44] In cell lysates, this antibody detected an APP protein product generated from cells expressing APP-FL that is consistent in size with full-length APP, as well as an APP protein that is consistent in size with the CTF that is expected if the protein is cleaved by α- or β-secretases (Figure 1D, left). The full-length APP protein and the CTF peptide are detected only in the cell lysate and not in the culture media using the C-terminal antibody (Figure 1D, right). Cells expressing APPΔex17 produced an APP protein migrating faster than the APP-FL protein, consistent with the deletion of 49 amino acids encoded by exon 17. No APP cleavage products were detected from cells expressing APPΔex17, suggesting that this protein isoform is not cleaved by β-secretase. The APPΔex17 protein was detected both in the cell lysates and in the cell culture media using the C-terminal antibody, indicating release of the APPΔex17 isoform from cells and into the extracellular space (Figure 1D).

To confirm that APPΔex17 was not an integral membrane protein, we isolated membranes from HEK293T cells expressing either APP or APPΔex17 and assessed the presence of the proteins in either soluble or membrane fractions (Figure S1). Membranes were washed with sodium-carbonate to open vesicles and dissociate peripheral membrane proteins.[45] As expected, full-length APP was present in the membrane fraction, and, to a lesser degree, in the sodium carbonate soluble fraction (soluble 2), likely due to release of a small amount during conversion of membrane vesicles into sheets (Figure S1). In contrast, APPΔex17 was detectable in the soluble fractions only,

Please cite this article in press as: Chang et al., Targeting Amyloid-β Precursor Protein, *APP*, Splicing with Antisense Oligonucleotides Reduces Toxic Amyloid-β Production, Molecular Therapy (2018), https://doi.org/10.1016/j.ymthe.2018.02.029

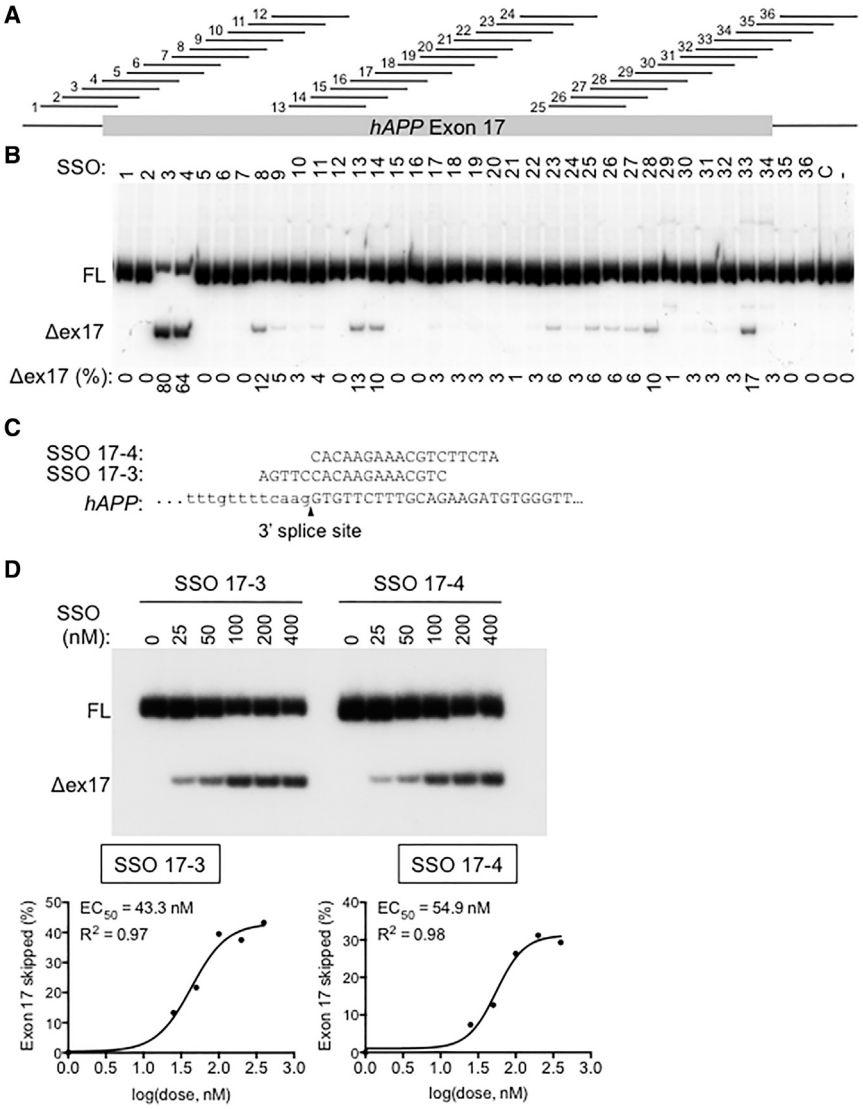

Figure 2. Splice-Switching Antisense Oligonucleotides Induce Human APP Exon 17 Skipping

(A) Diagram of SSO target sites on human APP exon 17 pre-mRNA. SSOs (horizontal lines) are numbered sequentially from the 5′ to 3′ end of the target region. Gray box indicates exonic region and lines are introns. (B) Radiolabeled RT-PCR analysis of RNA from HEK293T cells transfected with individual SSOs shown in (A). FL denotes APP mRNA with exon 17 and Δ17 denotes mRNA lacking exon 17 (skipped). Numbers above gel image designate SSO number and quantification of exon skipping (Δ17 /(Δ17 + FL)*100) is shown below gel. "C" indicates a sample from vehicle-treated control cells, and "–" represents untreated cells. (C) Alignment of the most active SSOs (17-3 and 17-4) with the target region of hAPP. Exonic and intronic sequences are depicted in capital and lowercase letters, respectively. The 3′ splice site cleavage site is denoted. (D) RT-PCR analysis of APP mRNA from HEK293T cells treated with increasing concentrations of SSO 17-3 and 17-4. Graphs show quantitation of exon 17 skipping, and the half-maximal effective concentration (EC_{50}) was calculated.

with no detectable signal in the membrane fraction. The bulk of APPΔex17 is found in the first soluble fraction, while the remaining protein is released from membranes during the sodium carbonate wash, suggesting that some protein either remained membrane associated through interactions with other membrane components or was contained within small vesicles that were not sheared during the initial fractionation. Regardless, the absence of APPΔex17 from the membrane fractions in this case suggests that it is not an integral membrane protein.

To determine whether Aβ was produced from APPΔex17, we used an Aβ42 ELISA to quantify abundance of the peptide in the culture media of cells transfected with the APP-FL or APPΔex17 expression plasmid. Aβ42 levels were high in the supernatant of cells expressing APP-FL and absent in the media of cells expressing APPΔex17, indicating that Aβ42 is not produced from APPΔex17 (Figure 1E).

SSOs Induce APP Exon 17 Skipping

An APP isoform lacking exon 17 does not produce the toxic Aβ42 peptide and thus, inducing the production of this isoform may be an effective way to lower Aβ42 and ultimately reduce Aβ plaque formation. To this end, we designed SSOs to block splicing of exon 17 and induce skipping of the exon in the APP mRNA. The SSOs are 2′-*O*-methoxyethyl (2′MOE)/phosphorothioate (PS) modified 18-mers that base-pair with the targeted pre-mRNA sequence and create a steric block to the spliceosome, thereby disrupting splicing.[35] We tested a series of 36 18-mer SSOs, tiled along the intron/exon 17 region such that each subsequent SSO overlapped the preceding SSO by five nucleotides (Figure 2A). Each SSO was individually transfected into HEK293T cells, and RNA was isolated 48 hr later and analyzed for APP exon 17 splicing by RT-PCR. SSOs 17-3 and 17-4 were the most active at inducing exon 17 skipping (Figure 2B). Both SSOs base pair at the 3′ splice site, likely causing exon 17 skipping by blocking spliceosomal recognition of the site (Figure 2C). The SSOs induce exon skipping in a dose-dependent manner with half-maximal effective activities (EC_{50}) of 43.3 and 54.9 nM, respectively (Figure 2D).

SSO-Mediated Exon 17 Skipping Reduces Aβ42 in Down Syndrome Patient Fibroblast Cells

To test whether SSOs that cause exon 17 skipping can lower Aβ42 abundance in a pathological model system *in vitro*, we assessed APP expression in fibroblasts from Down syndrome individuals. Down syndrome/Trisomy 21 (DS) cells have three copies of APP

Please cite this article in press as: Chang et al., Targeting Amyloid-β Precursor Protein, *APP*, Splicing with Antisense Oligonucleotides Reduces Toxic Amyloid-β Production, Molecular Therapy (2018), https://doi.org/10.1016/j.ymthe.2018.02.029

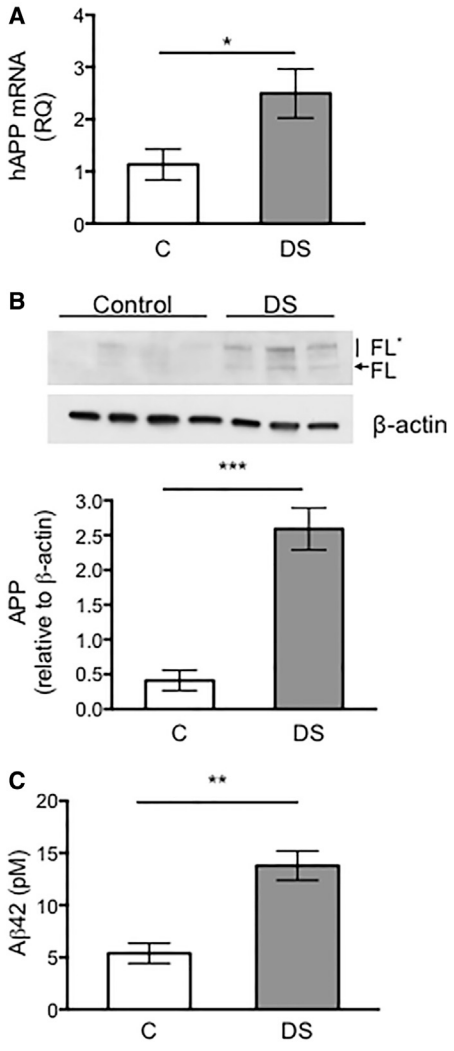

Figure 3. APP mRNA, Protein, and Aβ42 Levels Are Elevated in Down Syndrome Fibroblast Cells

(A) qPCR analysis of APP mRNA from DS (n = 4) and non-DS (n = 5) human fibroblast cells normalized to β-actin. Graph depicts the mean relative quantity (RQ) of APP (±SEM, *p < 0.05, unpaired, two-tailed Student's t test). (B) Representative immunoblot of APP overexpression in DS (n = 3) and control non-DS cell lines (n = 4) using an antibody that detects the N terminus of APP. FL* designates full-length mature APP (N- and O-glycosylation), and FL represents full-length immature APP (N-glycosylation). Quantitation of all forms of APP is shown in graph (±SEM, ***p < 0.001, unpaired, two-tailed Student's t test). (C) Quantitation of Aβ42 in control (n = 2) and DS fibroblast (n = 4) cell lines by ELISA. Graph depicts mean ±SEM (**p < 0.01, unpaired, two-tailed Student's t test).

due to the triplication of chromosome 21 and thus are a relevant model for APP overexpression and elevated Aβ42 levels. First, we analyzed APP mRNA expression in a number of different DS and non-DS control (C) cell lines and determined that APP mRNA was more than two times more abundant in DS fibroblast cell lines compared to control fibroblast cells (Figure 3A). The increase in mRNA abundance in DS cells relative to non-DS cells correlated with an increase in APP protein abundance in these cells (Figure 3B). Quantitation of Aβ42 by ELISA of the culture media revealed a significant elevation of Aβ42 levels in the DS fibroblast cells compared to non-DS cells (Figure 3C).

Next, we analyzed APP mRNA and protein expression in DS cells following transfection with increasing amounts of SSO 17-3. SSO 17-3 induced a dose-dependent decrease in full-length APP mRNA and an increase in APPΔex17 mRNA, with an EC_{50} of 12.2 nM (Figure 4A). Immunoblot analysis of APP protein in lysates from cells transfected with SSO 17-3 revealed a lower migrating band consistent with the expected size of APPΔex17 (Figure 4B). As expected, full-length APP protein levels were reduced and APPΔex17 protein increased (Figure 4C, top), but total APP protein abundance did not change with SSO treatment (Figure 4C, bottom).

Importantly, SSO 17-3 reduced and normalized Aβ42 peptide levels in the culture media from DS fibroblasts compared to media from cells treated with a control, untargeted SSO (SSO-C) (Figure 4D). Specifically, SSO 17-3 treatment resulted in a 45% decrease in Aβ42 in the media of DS cells, bringing Aβ42 to a level that was not significantly different than the level in karyotypically normal cells (Figure 4D). Together, these results demonstrate that SSO-induced skipping of APP exon 17 lowers Aβ concentration in DS cells without affecting overall APP protein levels.

SSO-Induced Exon Skipping Decreases Aβ Abundance in Mice

To test whether SSOs targeting APP splicing can lower Aβ *in vivo*, we designed SSOs targeted to the murine APP exon 15, which is homologous to human APP exon 17 and encodes the γ-cleavage sites. SSOs were first screened for activity *in vitro* in a mouse kidney cell line (Figure 5A).[46] We identified several SSOs that induced exon 15 skipping. The most active, SSO 15-3 and 15-31, resulted in 35% and 55% APP mRNA with exon 15 skipped, respectively (Figure 5B). SSO 15-3 base pairs at the 3′ splice site and 15-31 at the 5″ splice site of exon 15 (Figure 5C). Both SSOs induce exon 15 splicing in a dose-dependent manner (Figure 5D). SSO 15-31 treatment resulted in the most exon 15 skipping and was used in subsequent experiments.

To test SSO 15-31 activity *in vivo*, we administered the SSO to wild-type mice by i.c.v. injection. Neonate pups were injected with 25 or 50 μg of SSO 15-31 or a SSO-C at post-natal day 1 or 2 (P1–P2) and cortex, and hippocampus were collected from the mice 3 weeks later (Figure 6A). RT-PCR analysis of the RNA isolated from the tissues demonstrated significant APP exon 15 skipping in both regions of the brain from mice treated with SSO 15-31. There was a subtle increase in skipping in mice treated with 50 μg of ASO compared to the 25-μg dose (Figure 6B). To assess SSO distribution in the brain, we visualized SSO- and saline-treated tissue slices by immunohistochemistry using an antibody that specifically detects the antisense oligonucleotide.[47] We observed widespread distribution of SSO in the hippocampus (Figure 6C) and cortex (Figure 6D) of 3-week old mice that were treated with SSO as neonates and prominent

Please cite this article in press as: Chang et al., Targeting Amyloid-β Precursor Protein, *APP*, Splicing with Antisense Oligonucleotides Reduces Toxic Amyloid-β Production, Molecular Therapy (2018), https://doi.org/10.1016/j.ymthe.2018.02.029

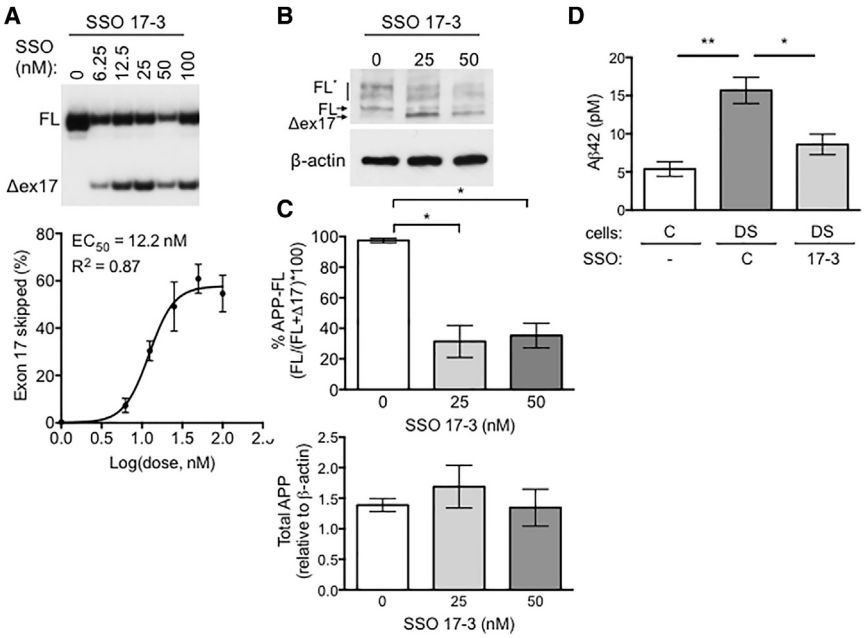

Figure 4. SSO-Induced APP Exon 17 Skipping Reduces Aβ42 in DS Cells

(A) RT-PCR analysis of APP mRNA from a representative DS patient fibroblast cell line (GM02767) treated with increasing concentrations of SSO 17-3. Graph represents the percent of APP mRNA that lacks exon 17 (exon 17 skipped [%]) related to the log of the SSO dose. The half-maximal effective concentration (EC_{50}) is shown. Error bars are SEM, n = 3 different DS cell lines. (B) Representative immunoblot analysis of SSO dose response in DS fibroblast cell lysates. β-actin was measured as a loading reference. FL* designates full-length mature APP (N + O glycosylation), and FL represents full-length immature APP (N glycosylation). Δex17 indicates the exon 17 skipped isoform. (C) Graphs display quantitation of the percent of all APP protein isoforms that is FL or FL* (top) and the amount of all APP protein isoforms, shown as the ratio of APP to β-actin (bottom). One-way ANOVAs with Tukey's post-test (n = 3 different DS cell lines) showed no significant difference in APP among the samples. Error bars are ±SEM. (D) ELISA analysis of Aβ42 secreted from control (C), non-DS untreated (–, n = 2) and DS fibroblast cell line treated with a control SSO (C, n = 4) or SSO 17-3 (n = 4). Error bars are ±SEM. One-way ANOVA with Tukey's multiple comparisons test (*$p < 0.05$, **$p < 0.01$).

co-localization of the SSO with the neuronal protein NeuN as well as in other non-neuronal cell types.

To determine whether SSO 15-31-induced APP exon 15 skipping can lower Aβ42 *in vivo*, we treated P1 mice with SSO 15-31 or SSO-C by i.c.v. injection and collected brain tissue 3 months later, a time point which should be sufficient to allow some normal accumulation of Aβ in wild-type mice and would also test the duration of SSO activity (Figure 7A).[48,49] We first confirmed that SSO is still present in the hippocampus and cortex of 4-month-old mice that were injected a single time with SSO at P1 (Figure S3), which is consistent with previous reports using ASOs.[38] The SSO did not have any overt adverse effects on the mice. Weights did not differ significantly between SSO 15-31- and SSO-C-treated animals (Figure S2A). There was also no evidence of endoplasmic reticulum (ER) stress from expression of the APP isoform as indicated by the absence of XBP1 splicing, which occurs as a part of the unfolded protein response[50] (Figure S2B), and there was no change in glial fibrillary acidic protein (GFAP) or allograft inflammatory factor 1 (AIF1) expression, which would indicate astrogliosis or microgliosis, respectively (Figure S2C).

Remarkably, RT-PCR analysis of RNA collected from cortical tissue showed APP exon 15 skipping at a similar level to that seen from samples collected 3 weeks after treatment, indicating a long-term, sustained effect of the SSO (Figures 7B and 7C). ELISA analysis of hippocampal samples revealed that SSO 15-31 treatment resulted in a 57% reduction in Aβ42 compared to mice treated with SSO-C (Figure 7D). These results indicate that sustained SSO-induced exon skipping that eliminates APP cleavage required to generate Aβ is an effective approach for lowering Aβ42 production *in vivo*.

These results demonstrate the long-term effects of SSO treatment on Aβ42 levels when treatment begins at birth. However, an AD therapeutic would likely be administered in adulthood. Thus, we tested SSO 15-31 activity in adult mice treated at 2 months of age by i.c.v. injection (Figure 8A). The hippocampus and cortex were collected 3 weeks after treatment for analysis. Similar to results with neonatal treatment, SSO administration to adult mice resulted in exon 15 skipping (Figures 8B and 8C) and a significant reduction in Aβ42 compared to mice treated with SSO-C (Figure 8D).

DISCUSSION

Aberrant *APP* expression and Aβ production has been implicated in many forms of dementia, including eFAD/EOAD, DS/Ts21, LOAD, and TBI. Hence, a method to lower Aβ is a promising therapeutic approach for these conditions. Here, we demonstrate that an isoform of the human APP protein that lacks exon 17, APPΔEx17, does not produce the toxic Aβ peptide (Figure 1). The APPΔEx17 isoform can be induced in cells using an SSO, SSO 17-3, that base pairs at the 3′ splice site of the exon, blocks splicing at the site and redirects splicing to exon 18, effectively removing exon 17 from the mRNA (Figure 2). We show that treatment with SSO 17-3 lowers full-length APP mRNA and normalizes Aβ42 production in Down syndrome patient fibroblast cell lines (Figure 4), which overexpress APP and consequently overproduce Aβ (Figure 3). We further demonstrate that a similar SSO, targeting mouse APP, can induce exon skipping in mice (Figures 5 and 6) and reduce Aβ42 abundance *in vivo* (Figures 7 and 8). Together, this study introduces a new antisense strategy to reduce the production of the Aβ peptide that is implicated in the pathology and progression of forms of dementia associated with APP mutations in familial AD, APP triplication in DS, as well as with sporadic AD.

Please cite this article in press as: Chang et al., Targeting Amyloid-β Precursor Protein, *APP*, Splicing with Antisense Oligonucleotides Reduces Toxic Amyloid-β Production, Molecular Therapy (2018), https://doi.org/10.1016/j.ymthe.2018.02.029

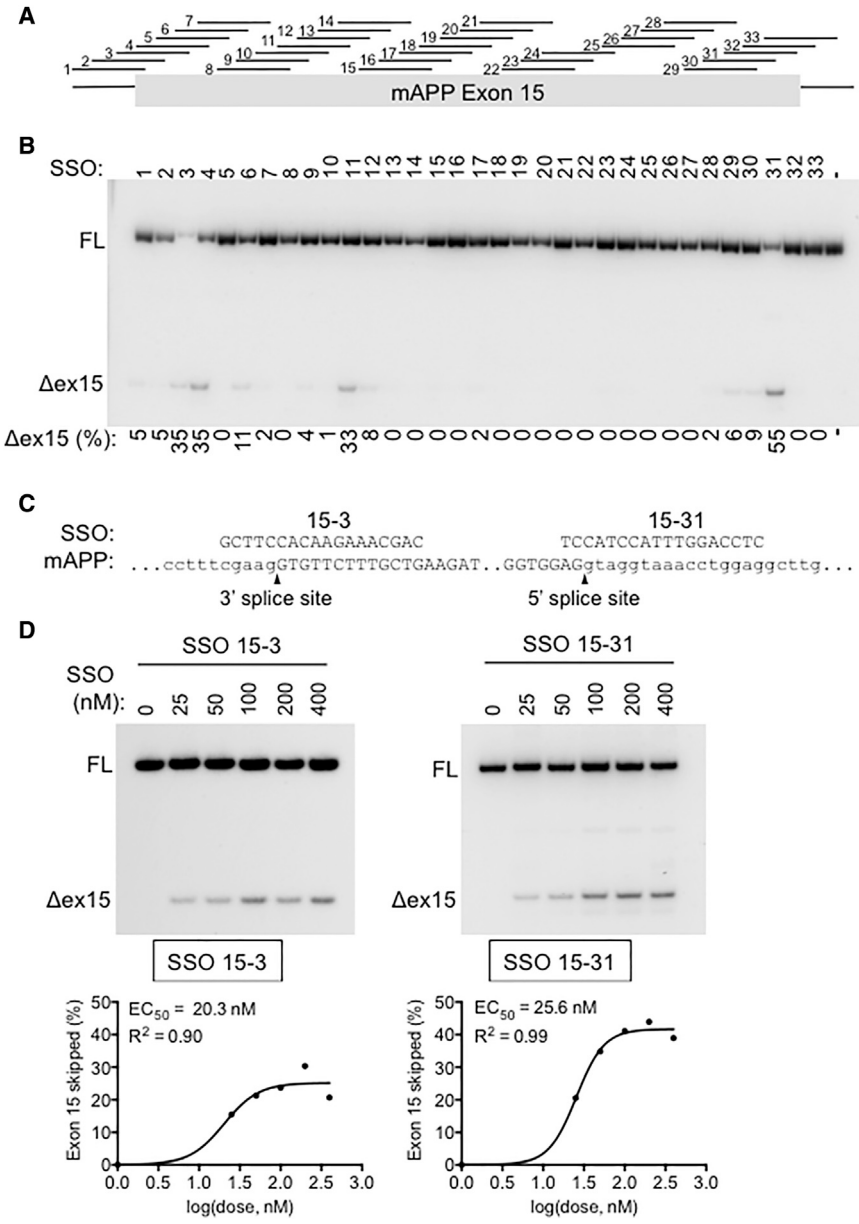

Figure 5. SSOs Induce Skipping of Murine APP Exon 15 Encoding the γ-Secretase Cleavage Sites

(A) Diagram of SSO target sites in the mouse APP exon 15 region, equivalent to human APP exon 17. SSOs (horizontal lines) are numbered sequentially from the 5′ to 3′ end of the target sequence. The gray box indicates the exonic region of exon 15, and lines adjacent represent introns. (B) Radiolabeled RT-PCR analysis of mRNA isolated from a mouse kidney cell line (208ee) transfected with individual SSOs shown in (A). FL designates full-length mAPP with exon 15 included, and Δex15 is mRNA lacking exon 15 (skipped). Numbers above gel image designate SSO number or untreated control (–), and quantification of exon skipping (% skipped = (Δex15/(Δex15+FL)*100) is shown below. (C) SSO 15-3 and 15-31 sequences aligned to target region of *mAPP*. Exonic and intronic sequences are depicted in capital and lowercase letters, respectively. (D) RT-PCR analysis of *mAPP* mRNA from mouse cells treated with increasing concentrations of SSO 15-3 or SSO 15-31. Graph represents the percent of APP mRNA that lacks exon 15 related to the log of the SSO dose. The potency of each SSO was determined using the half-maximal effective concentration (EC_{50}).

Overwhelming genetic evidence supports a causative role for Aβ accumulation in the initial stages of AD pathogenesis.[51,52] Currently, there are more than 50 different mutations in *APP* that are associated with AD (http://www.molgen.ua.ac.be/ADMutations).[53] The most common AD-associated *APP* mutation, V717I, results in an increase of the Aβ42 peptide.[54] Less common *APP* mutations are also associated with an increase in production of Aβ42. In addition, more than 200 *PSEN1* or *PSEN2* mutations have been identified in early onset AD, which lead to the overproduction of Aβ42.[53] Furthermore, a mutation in *APP* that lowers Aβ cleavage efficiency protects against the development of AD.[28] A role for APP in AD is further suggested by the prevalence of AD in DS/Trisomy 21, which constitutes the largest fraction of people with EOAD.[29] Rare cases of APP duplication in otherwise karyotypically normal individuals have also been associated with EOAD.[55,56] Similarly, DS individuals with partial trisomy of chromosome 21 that excluded APP did not develop EOAD and had no evidence of the plaques and tangles characteristic of the disease.[57,58] Other conditions also implicate APP expression in AD. For example, APP expression following TBI has been implicated in the development of AD.[31,59] Overall, the fact that EOAD, LOAD, DS, and TBI all have been associated with Aβ plaque pathology suggests the significance of APP dosage in AD pathology.

Despite clear evidence of a causative role for Aβ in AD, Aβ-mediated toxicity alone is insufficient to explain all facets of fully manifested AD.[52] Indeed, a recent report found that two familial AD mutations in PSEN1, PSEN-L435F and PSEN-C410Y, resulted in a dysfunctional protein that does not cleave APP, suggesting a possible Aβ-independent mechanism of AD.[60] However, follow-up experiments by Veugelen et al.,[61] demonstrated proteolytic activity from proteins with these mutations. Moreover, in these mutants, the loss of processive carboxypeptidase activity resulted in longer Aβ peptides, which are highly competent for seeding amyloid aggregates, consistent with *in vivo* observations of AD-related presenilin activity.[62]

Antisense strategies targeting APP expression *in vivo* have been previously explored.[63–65] For example, Kumar et al.[63] reported that administration of an APP-targeted ASO to mice lowers APP protein

Please cite this article in press as: Chang et al., Targeting Amyloid-β Precursor Protein, *APP*, Splicing with Antisense Oligonucleotides Reduces Toxic Amyloid-β Production, Molecular Therapy (2018), https://doi.org/10.1016/j.ymthe.2018.02.029

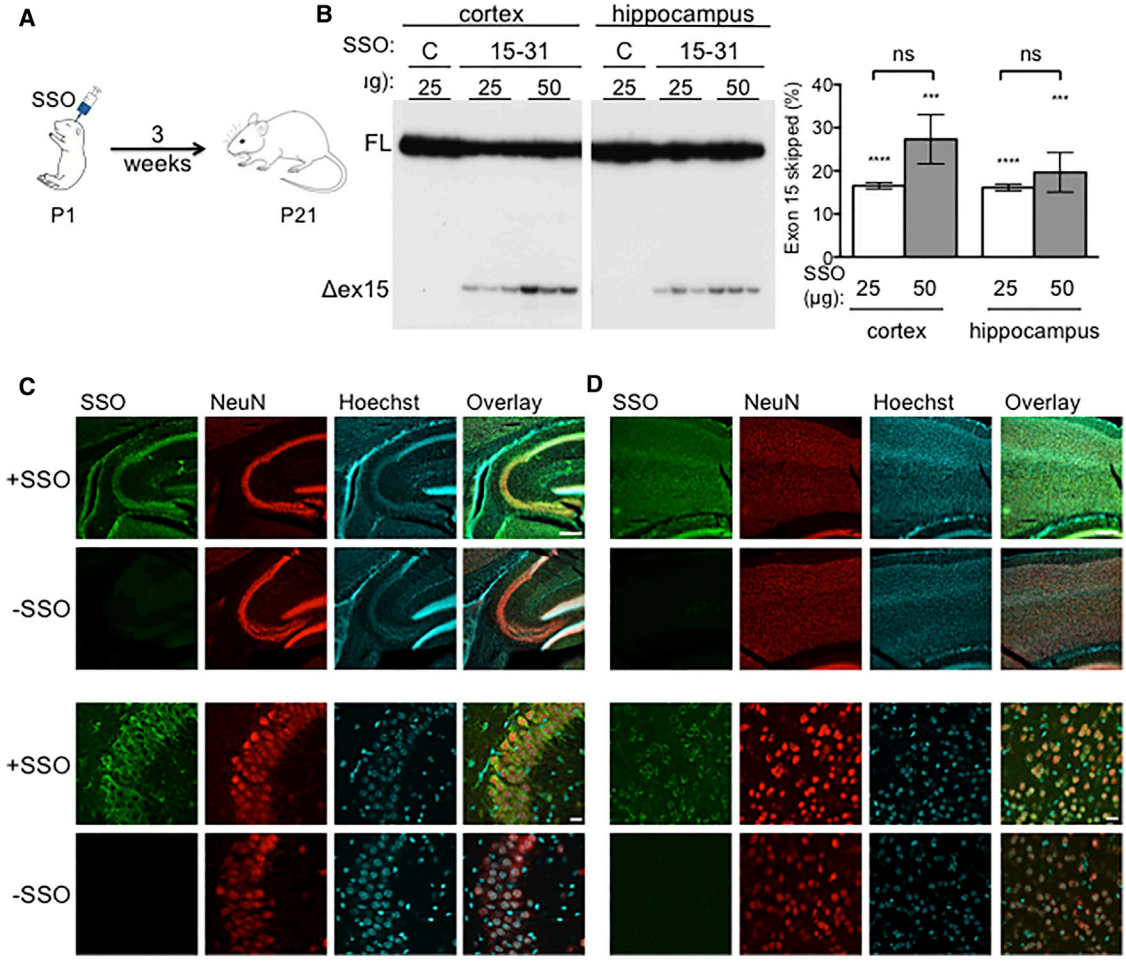

Figure 6. SSOs Induce APP Exon Skipping and Reduce Aβ42 Abundance *In Vivo*

(A) Schematic of experimental protocol with i.c.v. ASO administration at post-natal day 1 (P1) and analysis of ASO and splicing in tissue of treated mice 3 weeks later (P21). (B) Radiolabeled RT-PCR analysis of APP mRNA isolated from the cortex and hippocampus of mice (P21) that were injected at P1 or P2 with 25 or 50 μg of SSO 15-31. Graph depicts the mean ±SEM of exon 15 skipping (%) in indicated tissue from mice treated with SSO-C (n = 7) or SSO 15-31 (n = 9). Student's t test analysis indicated $p > 0.05$ between the two doses. Immunofluorescent microscopy images of SSO (green) in (C) hippocampus and (D) cortex (right) at 10× (top) and 60× (bottom) magnification from tissue isolated from mice injected with SSO 15-31 (+SSO) or saline vehicle (−SSO) and collected at P21. NeuN (red) marks neurons and Hoechst stain (blue) identifies nuclei. Scale bars in 10× = 220 μm; 60× = 20 μm.

and Aβ peptide levels and ameliorates physiological and behavioral pathology in animal models of aging and AD. However, it is important to note that ASOs used in previous studies are comprised, at least in part, of deoxynucleotides, which, upon base pairing to RNA create a substrate for RNase H, resulting in cleavage of the duplexed RNA and a predicted overall decrease in APP protein levels.[66] Our use of SSOs to induce APP alternative splicing and production of an mRNA that encodes an APP protein that cannot produce Aβ is a novel approach for downregulating APP and APP proteolysis that does not alter total APP protein levels.

The SSOs that we have designed induce skipping of the APP exon that encodes the cleavage sites necessary to generate toxic Aβ species. However, the majority of APP is intact in the APPΔex17 protein. Although the function of APP is not entirely clear, there is evidence to suggest that it acts as a receptor, given its similarities in structure to other type I transmembrane receptors as well as the discovery of receptor-like proteins that bind APP.[8,9,67] APP has also been implicated in cell adhesion.[68] Importantly, our antisense approach is aimed at downregulating pathological overexpression of APP in order to normalize APP levels and is not expected to produce a complete switch to the APPΔex17 protein isoform. Thus, there will be full-length APP available to perform important functions of the intact protein after SSO treatment. The homologs of APP, APLP1 and APLP2, will also likely offer some functional redundancy. One important factor in our approach is that the APPΔex17 protein does not appear to result in a gain of toxic function. We did not observe overt signs of toxicity in the SSO-treated

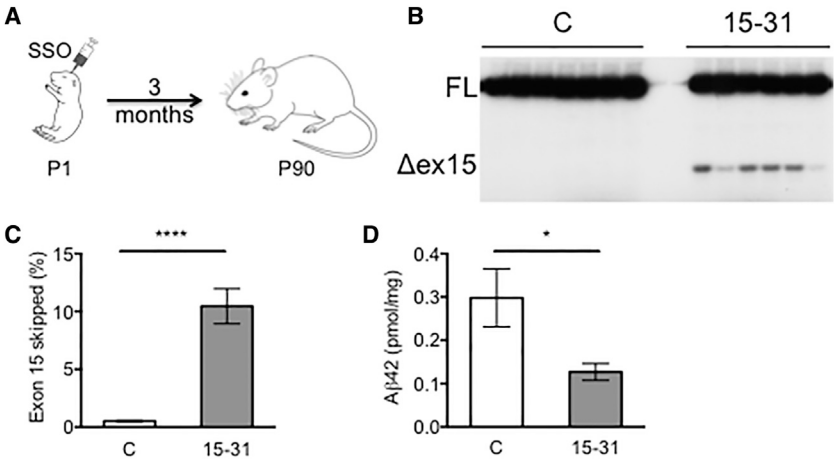

Figure 7. Long-Term Reduction of Aβ42 *In Vivo* following Treatment of Neonatal Mice with SSO 15-31

(A) Schematic of experimental protocol with i.c.v. ASO administration at P1 and analysis of splicing and Aβ42 in tissue from treated mice collected 3 months after treatment (P90). (B) Radiolabeled RT-PCR analysis of RNA isolated from the cortex of 3-month-old mice that were treated as neonates (P1/P2) with 25 μg of SSO-C (n = 8) or SSO 15-31 (n = 7). (C) Graph shows quantitation of *APP* exon 15 skipping in cortical tissue. Error bars are ±SEM, ****$p < 0.0001$, unpaired, two-tailed, Student's t test. (D) ELISA analysis of Aβ42 in the hippocampus from the same mice analyzed in (B) and (C). Graph represents the mean ±SEM, *$p < 0.05$, unpaired, two-tailed, Student's t test.

mice expressing APPΔex17 (Figure S2). In addition, we demonstrate that the APPΔex17 isoform is secreted into the culture media (Figure 1) and thus may preserve some of the functions of secreted APP, which have been reported to be neuroprotective and involved in the enhancement of long-term potentiation and memory.[69] More detailed studies investigating long-term effects of APPΔex17 expression *in vivo* will be needed to more definitively assess any potential toxic or beneficial affects associated with expression of the novel APP isoform.

AD treatments have struggled in clinical trials with few drugs advancing toward the market in the past 30 years. There are currently six FDA approved drugs for AD, though these treatments only temporarily improve symptoms and do not target the underlying causes of the disease that lead to fatal neurodegeneration.[3] There are a number of anti-amyloid antibodies in clinical development that have shown promise in clinical trials, further demonstrating the therapeutic value of targeting Aβ.[1,70] As an alternative to antibody and small-molecule therapeutic development, SSOs are a good platform for the treatment of neurological disorders, offering safe, long-lasting alterations in the gene expression following direct administration to the central nervous system.[36,38,66] Indeed, an SSO has recently been approved for the treatment of the fatal pediatric neurodegenerative disease spinal muscular atrophy (SMA).[40,71] The study presented here provides the basis for a therapeutic strategy for reduction of Aβ by modulation of APP pre-mRNA splicing to produce a cleavage-deficient protein isoform, offering an innovative approach for the treatment of AD.

MATERIALS AND METHODS

SSOs and Primers

All SSOs were uniformly modified with 2′-MOE and PS backbone as described previously.[72] A BLAST search for SSO 17-3 and SSO 15-31 complementary sequences identified no other sequence matches in the human or mouse genome. SSO-C also did not have any matches to genomic sequences. SSOs were formulated in sterile 0.9% saline. Primer and SSO sequences are provided in Table S1.

Expression Plasmids

The hAPP pCMV-AIP expression plasmid, used to produce human APP in culture, has been described elsewhere.[73] In brief, this plasmid co-expresses human APP with Swedish/Indiana mutations and a mutated form of presenilin (*PS1*DelE9) from a CMV promoter and produces both proteins through the use of an IRES sequence.[73] APPΔ17 was generated from this plasmid using the Q5 Site-Directed Mutagenesis Kit (New England BioLabs) to delete exon 17. The Δex17 construct was made using primer set AIPdeltaex17F and AIPdeltaex17R (Table S1). Deletion of exon 17 was confirmed by sequence analysis.

Cell Culture and Transfection

Individual SSOs targeting either human APP exon 17 or mouse APP exon 15 were transfected into HEK293T or a mouse primary kidney cell line (208ee),[74] respectively, at a final concentration of 100 nM. Cells were collected in TRIzol reagent (Life Technologies) 48 hr after transfection and analyzed for exon skipping.

DS fibroblasts (GM02571, GM02767, GM04928, AG04823, AG08942) along with chromosomally normal non-DS control fibroblast cell lines (GM03814, GM24590, GM24591, Coriell Cell Repository, and J-WT). SSOs for exon 17 skipping and control SSOs (final concentration 50 nM) were transfected into both DS and control non-DS fibroblasts and collected 48 hr after transfection. Three DS cell lines (GM02571, GM02767, GM04928) were analyzed for the dose response and immunoblot experiments. All cells were cultured in 10% fetal bovine serum (FBS) DMEM and maintained in a 37°C incubator with 5% CO_2 and transfected using Lipofectamine 2000 reagent (Life Technologies).

Mice

Mice (male and female C57BL/6J) (Jackson Laboratories) were bred, treated, and housed at Rosalind Franklin University of Medicine and Science. All animals were used and cared for in accordance with NIH guidelines and protocols reviewed and approved by the Institutional Animal Care and Use Committee at Rosalind Franklin University of Medicine and Science.

Please cite this article in press as: Chang et al., Targeting Amyloid-β Precursor Protein, *APP*, Splicing with Antisense Oligonucleotides Reduces Toxic Amyloid-β Production, Molecular Therapy (2018), https://doi.org/10.1016/j.ymthe.2018.02.029

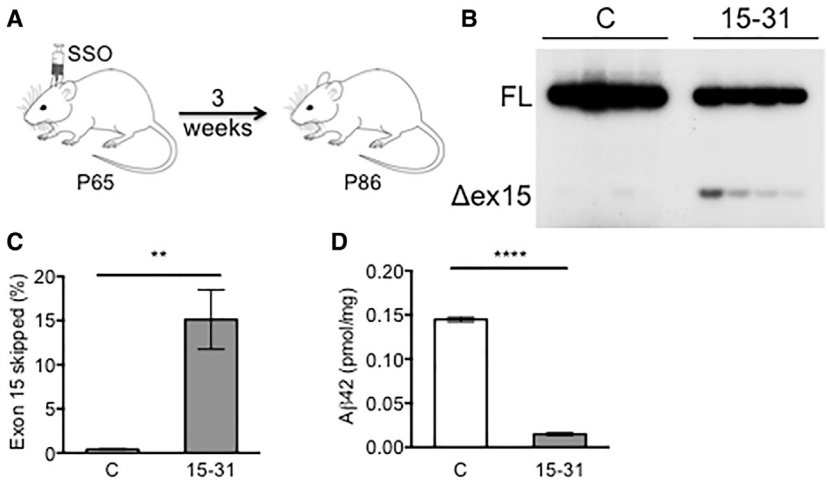

Figure 8. SSO 15-31 Reduces Aβ42 Abundance in Mice Treated as Adults

(A) Schematic of experimental protocol with i.c.v. ASO administration to adult mice (P65) and analysis of splicing and Aβ42 in tissue of treated mice 3 weeks after treatment (P86). (B) RT-PCR of RNA from mouse cortex 3 weeks post-treatment at 2 months of age. FL denotes full-length mAPP with exon 15 included, and Δex15 indicates transcripts with exon 15 skipped. (C) Quantitation of splicing from cortical tissue. Error bars are ±SEM. **$p < 0.01$, unpaired, two-tailed Student's t test. (D) Aβ42 ELISA analysis of adult i.c.v. mouse hippocampus treated with ASO 15-31 or vehicle control. Error bars are ±SEM. ****$p < 0.0001$, unpaired, two-tailed, Student's t test.

i.c.v. Injections

Neonatal mouse injections were performed as previously described.[38,46] In brief, neonatal mice were injected via i.c.v. injection with 25 or 50 μg of SSO 15-31 or SSO-C at P1 or P2. SSOs were diluted in sterile 0.9% saline with 0.01% Fast Green FCF, and 2.5 μL was injected into the left ventricle using a 33G needle fixed to a glass Hamilton syringe approximately 2.5 mm anterior to the lambda suture and 1 mm lateral to the sagittal suture to a depth of 2 mm. Brain tissue collection was performed on ice-cold PBS, and hippocampus and cortex tissue were either snap-frozen in liquid nitrogen or placed in 1 mL TRIzol reagent for immediate RNA extraction. RNA was extracted from tissues using TRIzol reagent (Life Technologies), and radioactive RT-PCR was performed using primers Mouse APP exon 14 F and Mouse APP exon 16 R (Table S1). Products were separated on a 6% non-denaturing polyacrylamide gel and quantified using a Typhoon 7000 phosphorimager (GE Healthcare).

For adult mouse i.c.v. injections, experiments were performed as previously described.[38] In brief, 3-month-old mice were secured in a stereotaxic frame and anesthetized with 2% isofluorine. A 10 μL Hamilton microsyringe with a 26G Huber point needle was used to administer 5 μL of SSO solution into the right lateral ventricle at 0.2 mm posterior and 1.0 mm lateral to the bregma lowered to a depth of 3 mm.

RT-PCR

RNA was extracted from tissue using TRIzol according to manufacturer's instructions. cDNA was generated using 1 μg of total RNA and GoScript Reverse Transcription System (Promega). Splicing was analyzed by radiolabeled PCR of cDNA using GoTaq Green (Promega) supplemented with α-^{32}P-deoxycytidine triphosphate (dCTP) and primers Human APP exon 14 F and Human APP exon 18 R flanking APP exon 15 and exon 18 (Table S1). Reaction products were run on a 6% non-denaturing polyacrylamide gel and quantified using a Typhoon 7000 phosphorimager (GE Healthcare).

Real-Time qPCR

cDNA extracted from the samples was analyzed via qPCR with SYBR Green PCR master mix (Life Technologies) using primers for APP normalized to human β-actin. All DS and control cell lines were run in two dilutions in triplicate in two separate experiments. Real-time PCR was performed on an Applied Biosystems (ABI) ViiA 7 Real-Time PCR System (through the Molecular Quantification Laboratory at RFUMS) according to manufacturer's protocols on Fast 96-well plates. Primers used were Human APP exon 14 F and Human APP exon 18 R (Table S1). The thermal-cycling protocol was as follows: stage 1 was 50°C for 2 min and 95°C for 10 min; stage 2 was 95°C for 15 s and 60°C for 1 min for 40 cycles to ensure an amplification plateau was reached. Taqman assay kits for mouse Aif1, mouse GFAP, and human β-actin were utilized (Mm00479862_g1, Mm01253033_m1, and 4352933E, respectively, Life Technologies). Results were analyzed with the ΔΔCT method.[75]

Immunoblot

For analysis of APP expression from expression plasmids, HEK293T cells were transfected with 1 μg of hAPP pCMV-AIP or pAPPΔex17. Forty hours post-transfection, cells were lysed in 150 mM NaCl, 5 0mM Tris-Cl (pH 7.4), 0.5% Na-DOC, 0.5% Triton X-100, 5 mM EDTA with protease inhibitors, and lysate was separated on 12% SDS-PAGE gels, or 8% SDS-PAGE gels for media samples, and transferred to polyvinylidene difluoride (PVDF) membranes. Membranes were probed with a rabbit polyclonal C-terminal APP antibody CTM-1 (1:4,000; a kind gift from Gopal Thinakaran) or a mouse monoclonal N-terminal APP antibody (1:1,000; Millipore 22C11) with appropriate HRP-linked secondary antibodies and exposed on an OmegaLum or Li-Cor imager.

For analysis of APP from DS cell cultures, cells were collected in 5× Laemmli buffer (25% glycerol, 12.5% 2-mercaptoethanol, 2.5% SDS, 0.02% bromophenol blue in 30% Tris buffer [0.5M Tris, 0.4% SDS, pH 6.8]) and boiled for 5 min at 100°C. Proteins were separated on 4%–15% Tris-glycine SDS-PAGE gradient gels (Bio-Rad),

transferred to PVDF membranes and probed with an antibody specific for the N or C terminus of APP (1:2,000; Abcam ab126732 and Millipore AB5352, respectively) and β-actin (1:5,000; Sigma A5441). Protein bands were quantified using ImageJ software (NIH). Three DS cell lines (GM02571, GM02767, GM04928) and control cell lines (GM03814, GM24590, GM24591, HL-WT) were used for this analysis.

For membrane isolation, subconfluent monolayers of HEK293T cells expressing APP or APPΔex17 were washed with phosphate-buffered saline with 5 mM EDTA and scraped into sucrose buffer (10 mM HEPES-KOH [pH 7.4], 10 mM KCl, 1.5 mM $MgCl_2$, 5 mM EDTA, 250 mM sucrose) and fractured by passing through a ball-bearing homogenizer (Isobiotech, Heidelberg, Germany) with an 8 micron clearance for 20 strokes. The solution was centrifuged at 1000 × *g* for 5 min to remove nuclei and other large debris, and the supernatant taken as the "Input" fraction. The input fraction was centrifuged at 20,000 × *g* for 1 hr to separate membranes from soluble components. The supernatant was taken as the "soluble" fraction and the membranes were resuspended in 100 mM sodium carbonate (pH 11.5) and incubated for 30 min at 4°C to open vesicles and remove peripheral membrane proteins.[45] The solution was then centrifuged at 20,000 × *g* for 1 hr and the supernatant taken as "soluble 2" while the pellet was resuspended in Laemmli sample buffer and labeled "membrane." Input fractions were assayed for protein concentration and loaded for Western analysis for equal concentration while other fractions were loaded as equal relative proportions of the input.

ELISA

Aβ-42 was measured using a Human/Rat β-Amyloid ELISA Kit (Wako) according to manufacturer's instructions. hAPP pCMV-AIP and hAPP pCMV-AIPΔ17 plasmids were transfected into HEK293T cells. Twenty-four hours post-transfection, culture media was removed, and cells were incubated in 2 mL of serum-free Opti-Mem media for 24 hr, at which time the media was collected and secreted Aβ42 was measured. All hAPP pCMV-AIP transfected samples were diluted (1:20) prior to analysis.

For analysis of Aβ produced from DS fibroblasts in culture, cells were plated onto 10-cm^2 tissue culture plates and transfected with either 50 nM of a control SSO or 50 nM of an SSO targeting skipping of APP exon 17 and allowed to incubate for 48 hr. Untreated controls to establish Aβ baseline production levels were not transfected with SSO. Subsequently, cells were cultured in 7 mL of serum-free Opti-Mem media for 5 days, and the media supernatant was collected. Aβ levels were measured from this collected media as described above and normalized to cellular protein abundance. For this experiment, cells were trypsinized off each plate and sonicated in 1 mL of RIPA buffer (10% sodium deoxycholate, 10% SDS, 0.5 M EDTA in PBS) supplemented with protease inhibitors (Sigma). Protein was collected and measured with a BCA Protein Assay Kit (Pierce). This experiment was repeated three times for each DS fibroblast line.

Analysis of Aβ in mouse tissue was performed as described previously.[46,76] In brief, frozen tissue was homogenized in a 5 M Guanidine-HCl solution. Supernatants were collected and diluted (1:10) for ELISA analysis. Protein concentration was measured via Bradford Protein Assay Kit (Pierce) and used to normalize Aβ concentration.

Immunohistochemistry

Mice treated with SSO or saline were anesthetized with 100 mg/mL urethane at 1 mg/g body weight and transcardially perfused with 1× PBS. Brains were removed, and one half was snap frozen in liquid nitrogen for use in RT-PCR analysis and the other half was fixed in 4% paraformaldehyde (PFA) and then moved to cold 30% sucrose after 48 hr. Sagittal sections (50 μm thick) were cut with a Leica SM 2010R. Slices were washed in wash solution (1× PBS with 0.1% Triton X-100) twice for 10 min, blocked with 4% goat serum in PBS for 2 hr at room temperature, and then incubated overnight at 4°C with primary antibodies against 2′-MOE SSOs (Ionis Pharmaceuticals, dilution 1:1,000) and NeuN (Millipore MAB377, dilution 1:1,000) in blocking buffer. The slices were washed with wash solution for 10 min three times and incubated for 2 hr at room temperature with secondary antibodies diluted in blocking buffer. Anti-rabbit (Alexa Fluor 488, 1:400) and anti-mouse (Alexa Fluor 594, 1:400) secondary antibodies were used. Sections were again washed in wash solution for three times for 10 min and then incubated for 10 min at room temperature with Hoechst stain (Thermo 33342, dilution 1:10,000 in 1× PBS) and mounted with Prolong Gold antifade reagent (Invitrogen). Sections were imaged using a Fluoview FV10 confocal microscope (Olympus).

Statistical Analysis

Statistics were performed using Prism 6 v. 6.0h. One-way ANOVA analysis with a post-hoc test (Tukey) was used to assess significant differences when comparing more than two groups. Student's t test, two-tailed, unpaired, was used to compare two groups. The specific statistical test used for each experiment is detailed in the figure legends.

SUPPLEMENTAL INFORMATION

Supplemental Information includes three figures and one table and can be found with this article online at https://doi.org/10.1016/j.ymthe.2018.02.029.

AUTHOR CONTRIBUTIONS

M.L.H. conceived the study. J.L.C., A.J.H., B.R., M.N., F.R., R.A.M., E.M.N., and M.L.H. designed and performed the experiments and analyzed the results. M.L.H. and J.L.C. wrote the paper with input from all the authors.

CONFLICTS OF INTEREST

F.R. is a paid employee of Ionis Pharmaceuticals (Carlsbad, CA).

ACKNOWLEDGMENTS

We thank Francine Jodelka for technical assistance and Gopal Thinakaran for the CTM-1 antibody. This work was financially supported by RFUMS internal research funding and NIH S10 OD 010662.

REFERENCES

1. Scheltens, P., Blennow, K., Breteler, M.M., de Strooper, B., Frisoni, G.B., Salloway, S., and Van der Flier, W.M. (2016). Alzheimer's disease. Lancet *388*, 505–517.
2. Prince, M., Bryce, R., Albanese, E., Wimo, A., Ribeiro, W., and Ferri, C.P. (2013). The global prevalence of dementia: a systematic review and metaanalysis. Alzheimers Dement. *9*, 63–75.e2.
3. Alzheimer's Association (2016). 2016 Alzheimer's disease facts and figures. Alzheimers Dement. *12*, 459–509.
4. Tcw, J., and Goate, A.M. (2017). Genetics of β-amyloid precursor protein in Alzheimer's disease. Cold Spring Harb. Perspect. Med. *7*, a024539.
5. Benilova, I., Karran, E., and De Strooper, B. (2012). The toxic Aβ oligomer and Alzheimer's disease: an emperor in need of clothes. Nat. Neurosci. *15*, 349–357.
6. Selkoe, D.J., and Hardy, J. (2016). The amyloid hypothesis of Alzheimer's disease at 25 years. EMBO Mol. Med. *8*, 595–608.
7. Karch, C.M., Cruchaga, C., and Goate, A.M. (2014). Alzheimer's disease genetics: from the bench to the clinic. Neuron *83*, 11–26.
8. Müller, U.C., Deller, T., and Korte, M. (2017). Not just amyloid: physiological functions of the amyloid precursor protein family. Nat. Rev. Neurosci. *18*, 281–298.
9. Dawkins, E., and Small, D.H. (2014). Insights into the physiological function of the β-amyloid precursor protein: beyond Alzheimer's disease. J. Neurochem. *129*, 756–769.
10. Zheng, H., and Koo, E.H. (2011). Biology and pathophysiology of the amyloid precursor protein. Mol. Neurodegener. *6*, 27.
11. Dyrks, T., Weidemann, A., Multhaup, G., Salbaum, J.M., Lemaire, H.G., Kang, J., Müller-Hill, B., Masters, C.L., and Beyreuther, K. (1988). Identification, transmembrane orientation and biogenesis of the amyloid A4 precursor of Alzheimer's disease. EMBO J. *7*, 949–957.
12. Kang, J., Lemaire, H.G., Unterbeck, A., Salbaum, J.M., Masters, C.L., Grzeschik, K.H., Multhaup, G., Beyreuther, K., and Müller-Hill, B. (1987). The precursor of Alzheimer's disease amyloid A4 protein resembles a cell-surface receptor. Nature *325*, 733–736.
13. Wasco, W., Bupp, K., Magendantz, M., Gusella, J.F., Tanzi, R.E., and Solomon, F. (1992). Identification of a mouse brain cDNA that encodes a protein related to the Alzheimer disease-associated amyloid beta protein precursor. Proc. Natl. Acad. Sci. USA *89*, 10758–10762.
14. Wasco, W., Gurubhagavatula, S., Paradis, M.D., Romano, D.M., Sisodia, S.S., Hyman, B.T., Neve, R.L., and Tanzi, R.E. (1993). Isolation and characterization of APLP2 encoding a homologue of the Alzheimer's associated amyloid beta protein precursor. Nat. Genet. *5*, 95–100.
15. Norstrom, E. (2017). Metabolic processing of the amyloid precursor protein—new pieces of the Alzheimer's puzzle. Discov. Med. *23*, 269–276.
16. Andrew, R.J., Kellett, K.A., Thinakaran, G., and Hooper, N.M. (2016). A Greek tragedy: the growing complexity of Alzheimer amyloid precursor protein proteolysis. J. Biol. Chem. *291*, 19235–19244.
17. Sisodia, S.S., Koo, E.H., Beyreuther, K., Unterbeck, A., and Price, D.L. (1990). Evidence that beta-amyloid protein in Alzheimer's disease is not derived by normal processing. Science *248*, 492–495.
18. Hardy, J., and Selkoe, D.J. (2002). The amyloid hypothesis of Alzheimer's disease: progress and problems on the road to therapeutics. Science *297*, 353–356.
19. Thinakaran, G., and Koo, E.H. (2008). Amyloid precursor protein trafficking, processing, and function. J. Biol. Chem. *283*, 29615–29619.
20. De Strooper, B., Iwatsubo, T., and Wolfe, M.S. (2012). Presenilins and γ-secretase: structure, function, and role in Alzheimer disease. Cold Spring Harb. Perspect. Med. *2*, a006304.
21. Takami, M., Nagashima, Y., Sano, Y., Ishihara, S., Morishima-Kawashima, M., Funamoto, S., and Ihara, Y. (2009). gamma-Secretase: successive tripeptide and tetrapeptide release from the transmembrane domain of beta-carboxyl terminal fragment. J. Neurosci. *29*, 13042–13052.
22. Chávez-Gutiérrez, L., Bammens, L., Benilova, I., Vandersteen, A., Benurwar, M., Borgers, M., Lismont, S., Zhou, L., Van Cleynenbreugel, S., Esselmann, H., et al. (2012). The mechanism of γ-secretase dysfunction in familial Alzheimer disease. EMBO J. *31*, 2261–2274.
23. Vassar, R., Kuhn, P.H., Haass, C., Kennedy, M.E., Rajendran, L., Wong, P.C., and Lichtenthaler, S.F. (2014). Function, therapeutic potential and cell biology of BACE proteases: current status and future prospects. J. Neurochem. *130*, 4–28.
24. De Strooper, B. (2014). Lessons from a failed γ-secretase Alzheimer trial. Cell *159*, 721–726.
25. Lanoiselée, H.M., Nicolas, G., Wallon, D., Rovelet-Lecrux, A., Lacour, M., Rousseau, S., Richard, A.C., Pasquier, F., Rollin-Sillaire, A., Martinaud, O., et al.; Collaborators of the CNR-MAJ project (2017). APP, PSEN1, and PSEN2 mutations in early-onset Alzheimer disease: a genetic screening study of familial and sporadic cases. PLoS Med. *14*, e1002270.
26. Marr, R.A., and Hafez, D.M. (2014). Amyloid-beta and Alzheimer's disease: the role of neprilysin-2 in amyloid-beta clearance. Front. Aging Neurosci. *6*, 187.
27. Karch, C.M., and Goate, A.M. (2015). Alzheimer's disease risk genes and mechanisms of disease pathogenesis. Biol. Psychiatry *77*, 43–51.
28. Jonsson, T., Atwal, J.K., Steinberg, S., Snaedal, J., Jonsson, P.V., Bjornsson, S., Stefansson, H., Sulem, P., Gudbjartsson, D., Maloney, J., et al. (2012). A mutation in APP protects against Alzheimer's disease and age-related cognitive decline. Nature *488*, 96–99.
29. Antonarakis, S.E. (2017). Down syndrome and the complexity of genome dosage imbalance. Nat. Rev. Genet. *18*, 147–163.
30. Castro, P., Zaman, S., and Holland, A. (2017). Alzheimer's disease in people with Down's syndrome: the prospects for and the challenges of developing preventative treatments. J. Neurol. *264*, 804–813.
31. Johnson, V.E., Stewart, W., and Smith, D.H. (2010). Traumatic brain injury and amyloid-β pathology: a link to Alzheimer's disease? Nat. Rev. Neurosci. *11*, 361–370.
32. Bird, S.M., Sohrabi, H.R., Sutton, T.A., Weinborn, M., Rainey-Smith, S.R., Brown, B., Patterson, L., Taddei, K., Gupta, V., Carruthers, M., et al. (2016). Cerebral amyloid-β accumulation and deposition following traumatic brain injury—a narrative review and meta-analysis of animal studies. Neurosci. Biobehav. Rev. *64*, 215–228.
33. Gaiteri, C., Mostafavi, S., Honey, C.J., De Jager, P.L., and Bennett, D.A. (2016). Genetic variants in Alzheimer disease—molecular and brain network approaches. Nat. Rev. Neurol. *12*, 413–427.
34. Barnes, D.E., and Yaffe, K. (2011). The projected effect of risk factor reduction on Alzheimer's disease prevalence. Lancet Neurol. *10*, 819–828.
35. Havens, M.A., Duelli, D.M., and Hastings, M.L. (2013). Targeting RNA splicing for disease therapy. Wiley Interdiscip. Rev. RNA *4*, 247–266.
36. Havens, M.A., and Hastings, M.L. (2016). Splice-switching antisense oligonucleotides as therapeutic drugs. Nucleic Acids Res. *44*, 6549–6563.
37. Bennett, C.F., Baker, B.F., Pham, N., Swayze, E., and Geary, R.S. (2017). Pharmacology of antisense drugs. Annu. Rev. Pharmacol. Toxicol. *57*, 81–105.
38. Rigo, F., Chun, S.J., Norris, D.A., Hung, G., Lee, S., Matson, J., Fey, R.A., Gaus, H., Hua, Y., Grundy, J.S., et al. (2014). Pharmacology of a central nervous system delivered 2′-O-methoxyethyl-modified survival of motor neuron splicing oligonucleotide in mice and nonhuman primates. J. Pharmacol. Exp. Ther. *350*, 46–55.
39. McClorey, G., and Wood, M.J. (2015). An overview of the clinical application of antisense oligonucleotides for RNA-targeting therapies. Curr. Opin. Pharmacol. *24*, 52–58.
40. Wan, L., and Dreyfuss, G. (2017). Splicing-correcting therapy for SMA. Cell *170*, 5.
41. Hua, Y., Sahashi, K., Rigo, F., Hung, G., Horev, G., Bennett, C.F., and Krainer, A.R. (2011). Peripheral SMN restoration is essential for long-term rescue of a severe spinal muscular atrophy mouse model. Nature *478*, 123–126.
42. Glascock, J., Lenz, M., Hobby, K., and Jarecki, J. (2017). Cure SMA and our patient community celebrate the first approved drug for SMA. Gene Ther. *24*, 498–500.

43. Rohn, T.T., Ivins, K.J., Bahr, B.A., Cotman, C.W., and Cribbs, D.H. (2000). A monoclonal antibody to amyloid precursor protein induces neuronal apoptosis. J. Neurochem. *74*, 2331–2342.

44. Vetrivel, K.S., Meckler, X., Chen, Y., Nguyen, P.D., Seidah, N.G., Vassar, R., Wong, P.C., Fukata, M., Kounnas, M.Z., and Thinakaran, G. (2009). Alzheimer disease Abeta production in the absence of S-palmitoylation-dependent targeting of BACE1 to lipid rafts. J. Biol. Chem. *284*, 3793–3803.

45. Fujiki, Y., Hubbard, A.L., Fowler, S., and Lazarow, P.B. (1982). Isolation of intracellular membranes by means of sodium carbonate treatment: application to endoplasmic reticulum. J. Cell Biol. *93*, 97–102.

46. Hinrich, A.J., Jodelka, F.M., Chang, J.L., Brutman, D., Bruno, A.M., Briggs, C.A., James, B.D., Stutzmann, G.E., Bennett, D.A., Miller, S.A., et al. (2016). Therapeutic correction of ApoER2 splicing in Alzheimer's disease mice using antisense oligonucleotides. EMBO Mol. Med. *8*, 328–345.

47. Smith, R.A., Miller, T.M., Yamanaka, K., Monia, B.P., Condon, T.P., Hung, G., Lobsiger, C.S., Ward, C.M., McAlonis-Downes, M., Wei, H., et al. (2006). Antisense oligonucleotide therapy for neurodegenerative disease. J. Clin. Invest. *116*, 2290–2296.

48. Puzzo, D., Privitera, L., Fa', M., Staniszewski, A., Hashimoto, G., Aziz, F., Sakurai, M., Ribe, E.M., Troy, C.M., Mercken, M., et al. (2011). Endogenous amyloid-β is necessary for hippocampal synaptic plasticity and memory. Ann. Neurol. *69*, 819–830.

49. Miller, B.C., Eckman, E.A., Sambamurti, K., Dobbs, N., Chow, K.M., Eckman, C.B., Hersh, L.B., and Thiele, D.L. (2003). Amyloid-beta peptide levels in brain are inversely correlated with insulysin activity levels in vivo. Proc. Natl. Acad. Sci. USA *100*, 6221–6226.

50. Walter, P., and Ron, D. (2011). The unfolded protein response: from stress pathway to homeostatic regulation. Science *334*, 1081–1086.

51. Van Cauwenberghe, C., Van Broeckhoven, C., and Sleegers, K. (2016). The genetic landscape of Alzheimer disease: clinical implications and perspectives. Genet. Med. *18*, 421–430.

52. De Strooper, B., and Karran, E. (2016). The cellular phase of Alzheimer's disease. Cell *164*, 603–615.

53. Cruts, M., Theuns, J., and Van Broeckhoven, C. (2012). Locus-specific mutation databases for neurodegenerative brain diseases. Hum. Mutat. *33*, 1340–1344.

54. Chartier-Harlin, M.C., Crawford, F., Houlden, H., Warren, A., Hughes, D., Fidani, L., Goate, A., Rossor, M., Roques, P., Hardy, J., et al. (1991). Early-onset Alzheimer's disease caused by mutations at codon 717 of the beta-amyloid precursor protein gene. Nature *353*, 844–846.

55. Rovelet-Lecrux, A., Hannequin, D., Raux, G., Le Meur, N., Laquerrière, A., Vital, A., Dumanchin, C., Feuillette, S., Brice, A., Vercelletto, M., et al. (2006). APP locus duplication causes autosomal dominant early-onset Alzheimer disease with cerebral amyloid angiopathy. Nat. Genet. *38*, 24–26.

56. Sleegers, K., Brouwers, N., Gijselinck, I., Theuns, J., Goossens, D., Wauters, J., Del-Favero, J., Cruts, M., van Duijn, C.M., and Van Broeckhoven, C. (2006). APP duplication is sufficient to cause early onset Alzheimer's dementia with cerebral amyloid angiopathy. Brain *129*, 2977–2983.

57. Doran, E., Keator, D., Head, E., Phelan, M.J., Kim, R., Totoiu, M., Barrio, J.R., Small, G.W., Potkin, S.G., and Lott, I.T. (2017). Down syndrome, partial trisomy 21, and absence of Alzheimer's disease: the role of APP. J. Alzheimers Dis. *56*, 459–470.

58. Prasher, V.P., Farrer, M.J., Kessling, A.M., Fisher, E.M., West, R.J., Barber, P.C., and Butler, A.C. (1998). Molecular mapping of Alzheimer-type dementia in Down's syndrome. Ann. Neurol. *43*, 380–383.

59. Acosta, S.A., Tajiri, N., Sanberg, P.R., Kaneko, Y., and Borlongan, C.V. (2017). Increased amyloid precursor protein and Tau expression manifests as key secondary cell death in chronic traumatic brain injury. J. Cell. Physiol. *232*, 665–677.

60. Xia, D., Watanabe, H., Wu, B., Lee, S.H., Li, Y., Tsvetkov, E., Bolshakov, V.Y., Shen, J., and Kelleher, R.J., 3rd (2015). Presenilin-1 knockin mice reveal loss-of-function mechanism for familial Alzheimer's disease. Neuron *85*, 967–981.

61. Veugelen, S., Saito, T., Saido, T.C., Chávez-Gutiérrez, L., and De Strooper, B. (2016). Familial Alzheimer's disease mutations in presenilin generate amyloidogenic Aβ peptide seeds. Neuron *90*, 410–416.

62. Szaruga, M., Veugelen, S., Benurwar, M., Lismont, S., Sepulveda-Falla, D., Lleo, A., Ryan, N.S., Lashley, T., Fox, N.C., Murayama, S., et al. (2015). Qualitative changes in human γ-secretase underlie familial Alzheimer's disease. J. Exp. Med. *212*, 2003–2013.

63. Kumar, V.B., Farr, S.A., Flood, J.F., Kamlesh, V., Franko, M., Banks, W.A., and Morley, J.E. (2000). Site-directed antisense oligonucleotide decreases the expression of amyloid precursor protein and reverses deficits in learning and memory in aged SAMP8 mice. Peptides *21*, 1769–1775.

64. Chauhan, N.B., and Siegel, G.J. (2007). Antisense inhibition at the beta-secretase-site of beta-amyloid precursor protein reduces cerebral amyloid and acetyl cholinesterase activity in Tg2576. Neuroscience *146*, 143–151.

65. Chakravarthy, M., Chen, S., Dodd, P.R., and Veedu, R.N. (2017). Nucleic acid-based theranostics for tackling Alzheimer's disease. Theranostics *7*, 3933–3947.

66. Khvorova, A., and Watts, J.K. (2017). The chemical evolution of oligonucleotide therapies of clinical utility. Nat. Biotechnol. *35*, 238–248.

67. Deyts, C., Thinakaran, G., and Parent, A.T. (2016). APP receptor? To be or not to be. Trends Pharmacol. Sci. *37*, 390–411.

68. Stahl, R., Schilling, S., Soba, P., Rupp, C., Hartmann, T., Wagner, K., Merdes, G., Eggert, S., and Kins, S. (2014). Shedding of APP limits its synaptogenic activity and cell adhesion properties. Front. Cell. Neurosci. *8*, 410.

69. Mockett, B.G., Richter, M., Abraham, W.C., and Müller, U.C. (2017). Therapeutic potential of secreted amyloid precursor protein APPsα. Front. Mol. Neurosci. *10*, 30.

70. Sevigny, J., Chiao, P., Bussière, T., Weinreb, P.H., Williams, L., Maier, M., Dunstan, R., Salloway, S., Chen, T., Ling, Y., et al. (2016). The antibody aducanumab reduces Aβ plaques in Alzheimer's disease. Nature *537*, 50–56.

71. Hua, Y., Vickers, T.A., Baker, B.F., Bennett, C.F., and Krainer, A.R. (2007). Enhancement of SMN2 exon 7 inclusion by antisense oligonucleotides targeting the exon. PLoS Biol. *5*, e73.

72. Baker, B.F., Lot, S.S., Condon, T.P., Cheng-Flournoy, S., Lesnik, E.A., Sasmor, H.M., and Bennett, C.F. (1997). 2′-O-(2-Methoxy)ethyl-modified anti-intercellular adhesion molecule 1 (ICAM-1) oligonucleotides selectively increase the ICAM-1 mRNA level and inhibit formation of the ICAM-1 translation initiation complex in human umbilical vein endothelial cells. J. Biol. Chem. *272*, 11994–12000.

73. Singer, O., Marr, R.A., Rockenstein, E., Crews, L., Coufal, N.G., Gage, F.H., Verma, I.M., and Masliah, E. (2005). Targeting BACE1 with siRNAs ameliorates Alzheimer disease neuropathology in a transgenic model. Nat. Neurosci. *8*, 1343–1349.

74. Lentz, J.J., Jodelka, F.M., Hinrich, A.J., McCaffrey, K.E., Farris, H.E., Spalitta, M.J., Bazan, N.G., Duelli, D.M., Rigo, F., and Hastings, M.L. (2013). Rescue of hearing and vestibular function by antisense oligonucleotides in a mouse model of human deafness. Nat. Med. *19*, 345–350.

75. Livak, K.J., and Schmittgen, T.D. (2001). Analysis of relative gene expression data using real-time quantitative PCR and the 2(−Delta Delta C(T)) method. Methods *25*, 402–408.

76. Hafez, D.M., Huang, J.Y., Richardson, J.C., Masliah, E., Peterson, D.A., and Marr, R.A. (2012). F-spondin gene transfer improves memory performance and reduces amyloid-β levels in mice. Neuroscience *223*, 465–472.

YMTHE, Volume *26*

Supplemental Information

Targeting Amyloid-β Precursor Protein, *APP*, Splicing with Antisense Oligonucleotides Reduces Toxic Amyloid-β Production

Jennifer L. Chang, Anthony J. Hinrich, Brandon Roman, Michaela Norrbom, Frank Rigo, Robert A. Marr, Eric M. Norstrom, and Michelle L. Hastings

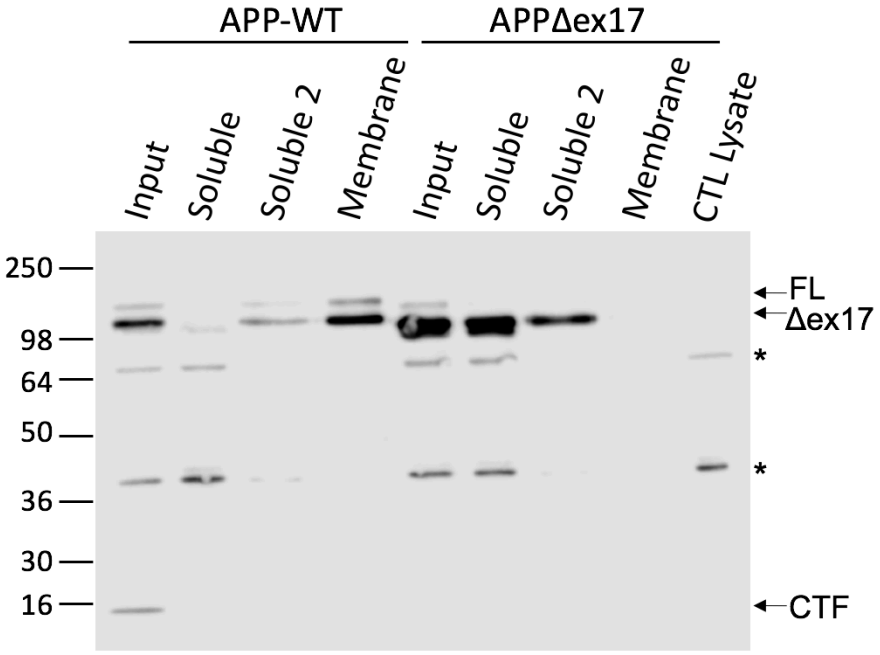

Figure S1. Immunoblot of APP with an antibody to detect the C-terminus of the protein in membrane and soluble fractions of cell lysates expressing APP-FL or APPΔex17 expression plasmids. Input refers to a sample prior to fractionation. FL full-length mature APP (FL), the protein generated from mRNA lacking exon 17 (Δex17), and the C-terminal fragment (CTF) that remains in cells after cleavage are labeled. * represents nonspecific protein bands. A sample with lysate from untransfected cells is included as a control (CTL).

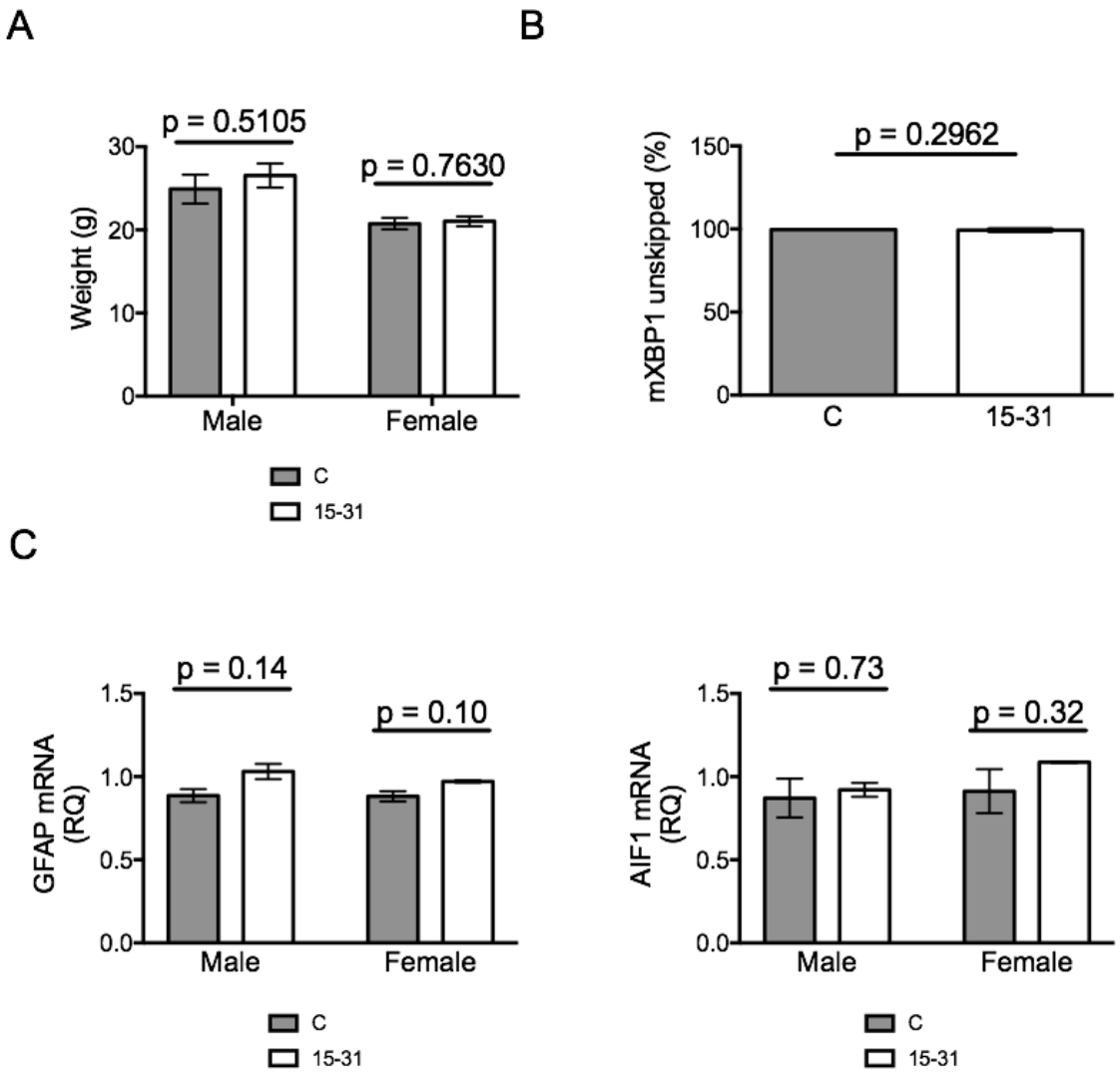

Figure S2. SSOs do not cause adverse side effects. (A) Weights of 3-month-old male and female mice treated with a control SSO (n = 3 male; 4 female) and SSO 15-31 (n = 3 male; 5 female) at P1. (B) RT-PCR analysis of mXBP1 mRNA splicing in tissue of 3-month-old mice that were treated by ICV with control SSO (C, n = 7) or 15-31 (n = 8) at P1. (C) Real-time quantitative PCR analysis of GFAP and AIF1 in mice described in (A) and (B). Error bars represent ± s.e.m.

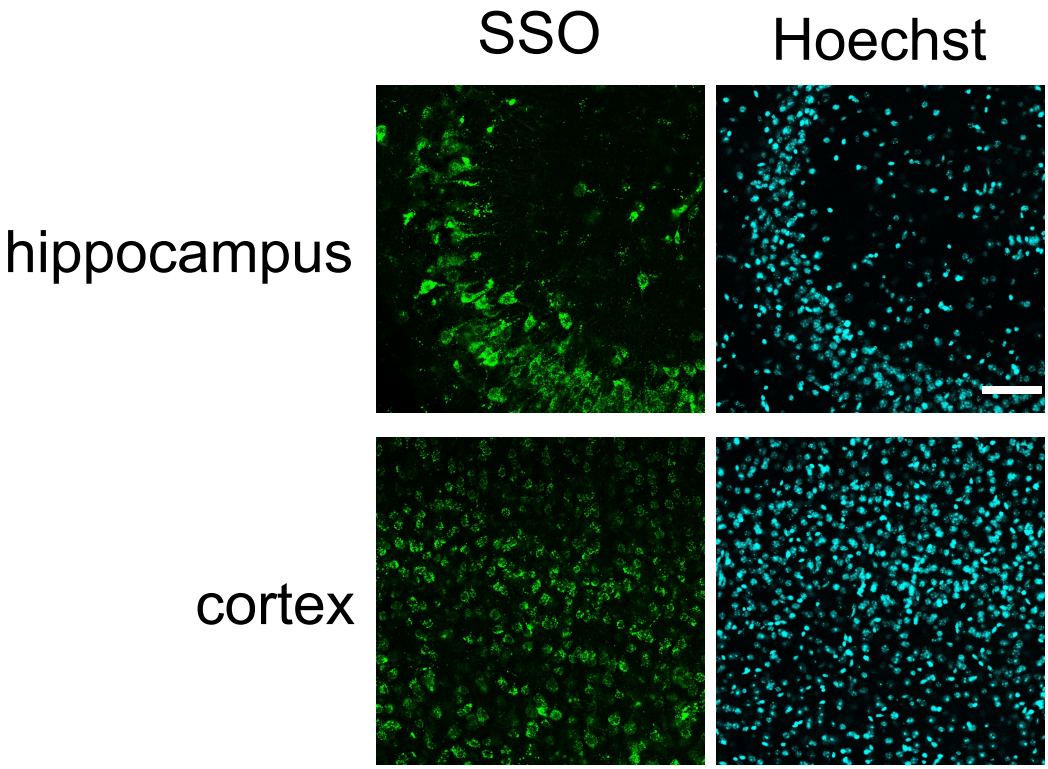

Figure S3. Immunofluorescent microscopy images of SSO (green) in hippocampus (top) cortex (bottom) at 20X magnification in tissue isolated from mice treated with SSO-C at P1 by ICV injection and collected at 4 months of age.[46] Hoechst stain (blue) identifies nuclei. Scale bars in 20X = 110 μm.

Table S1 – Splice switching Antisense Oligonucleotides and Primers

Human		Mouse	
SSOs	Sequence (5'-3')	**SSOs**	Sequence (5'-3')
1	CACCTTGAAAACAAATTA	1	CACCTTCGAAAGGAAGCC
2	AAGAACACCTTGAAAACA	2	AAGAACACCTTCGAAAGG
3	CTGCAAAGAACACCTTGA	3	CAGCAAAGAACACCTTCG
4	ATCTTCTGCAAAGAACAC	4	ATCTTCAGCAAAGAACAC
5	CCCACATCTTCTGCAAAG	5	CCCACATCTTCAGCAAAG
6	TTGAACCCACATCTTCTG	6	TCGAACCCACATCTTCAG
7	TTTGTTTGAACCCACATC	7	TTTGTTCGAACCCACATC
8	GCACCTTTGTTTGAACCC	8	GCGCCTTTGTTCGAACCC
9	TGATTGCACCTTTGTTTG	9	TGATGGCGCCTTTGTTCG
10	TCCAATGATTGCACCTTT	10	TCCGATGATGGCGCCTTT
11	ATGAGTCCAATGATTGCA	11	ATGAGTCCGATGATGGCG
12	CCACCATGAGTCCAATGA	12	CCACCATGAGTCCGATGA
13	ACCGCCCACCATGAGTCC	13	GCCGCCCACCATGAGTCC
14	ACAACACCGCCCACCATG	14	ACAACGCCGCCCACCATG
15	CTATGACAACACCGCCCA	15	CTATGACAACGCCGCCCA
16	TGTCGCTATGACAACACC	16	GGTTGCTATGACAACGCC
17	ATCACTGTCGCTATGACA	17	ATCACGGTTGCTATGACA
18	TGACGATCACTGTCGCTA	18	TGACAATCACGGTTGCTA
19	GGTGATGACGATCACTGT	19	GGTGATGACAATCACGGT
20	ACCAAGGTGATGACGATC	20	ACCAGGGTGATGACAATC
21	GCATCACCAAGGTGATGA	21	ACATCACCAGGGTGATGA
22	CTTCAGCATCACCAAGGT	22	CTTCAACATCACCAGGGT
23	TTCTTCTTCAGCATCACC	23	TTCTTCTTCAACATCACC
24	ACTGTTTCTTCTTCAGCA	24	ACTGTTTCTTCTTCAACA
25	TGTGTACTGTTTCTTCTT	25	GATGGATGGATGTGTACT
26	ATGGATGTGTACTGTTTC	26	GCCATGATGGATGGATGT
27	GATGAATGGATGTGTACT	27	ACCACGCCATGATGGATG
28	ACCATGATGAATGGATGT	28	CCTCCACCACGCCATGAT
29	ACCACACCATGATGAATG	29	ACCTACCTCCACCACGCC
30	CCTCCACCACACCATGAT	30	GGTTTACCTACCTCCACC
31	ACCTACCTCCACCACACC	31	CTCCAGGTTTACCTACCT
32	AGTTTACCTACCTCCACC	32	CAAGCCTCCAGGTTTACC
33	AGTCAAGTTTACCTACCT	33	GCAGACAAGCCTCCAGGT
34	CATGCAGTCAAGTTTACC		
35	GGAAACATGCAGTCAAGT		
36	CACTTGGAAACATGCAGT		
Primers	Sequence (5'-3')	Primers	Sequence (5'-3')
AIPdeltaex17F	GTTGACGCCGCTGTCACC	mAPP ex14 F	AGACGGAAGAGATCTCGG
AIPdeltaex17R	CAATTTTTGATGATGAACTTCATATCC	mAPP ex16 R	GGTCACGGCGGCGTCGAC
hAPP ex14F	CCAGCCAACACAGAAAACGAAG	mXBP1 F	ACACGCTTGGGAATGGACAC
hAPP ex18R	CTAGTTCTGCATCTGCTCAAAGAAC	mXBP1 R	CCATGGGAAGATGTTCTGGG
hXBP1 F	CCTTGTAGTTGAGAACCAGGAG	mGAPDH F	GTGAGGCCGGTGCTGAGTATG
hXBP1 R	GGTCCAAGTTGTCCAGAATGC	mGAPDH R	GCCAAAGTTGTCATGGATGAC
hACTB F	AAAGACCTGTACGCCAACAC		
hACTB R	GTCATACTCCTGCTTGCTGAT		